

## The chaperonin CCT promotes the formation of fibrillar aggregates of $\gamma$ -tubulin



Luis Pouchucq<sup>a,c</sup>, Pablo Lobos-Ruiz<sup>a</sup>, Gissela Araya<sup>a</sup>, José María Valpuesta<sup>b</sup>,  
Octavio Monasterio<sup>a,\*</sup>

<sup>a</sup> Laboratorio de Biología Estructural y Molecular, Departamento de Biología, Facultad de Ciencias, Universidad de Chile, Santiago, Chile

<sup>b</sup> Departamento de Estructura de Macromoléculas, Centro Nacional de Biotecnología (CNB-CSIC), Campus de la Universidad Autónoma de Madrid, 28049 Madrid, Spain

<sup>c</sup> Laboratorio de Biotecnología Vegetal Ambiental, Departamento de Biotecnología, Universidad Tecnológica Metropolitana, Santiago, Chile

### ARTICLE INFO

#### Keywords:

Electron microscopy

Folding

Chaperonin

Protein aggregation

TriC

TCP-1

### ABSTRACT

The type II chaperonin CCT is involved in the prevention of the pathogenesis of numerous human misfolding disorders, as it sequesters misfolded proteins, blocks their aggregation and helps them to achieve their native state. In addition, it has been reported that CCT can prevent the toxicity of non-client amyloidogenic proteins by the induction of non-toxic aggregates, leading to new insight in chaperonin function as an aggregate remodeling factor. Here we add experimental evidence to this alternative mechanism by which CCT actively promotes the formation of conformationally different aggregates of  $\gamma$ -tubulin, a non-amyloidogenic CCT client protein, which are mediated by specific CCT- $\gamma$ -tubulin interactions. The *in vitro*-induced aggregates were in some cases long fiber polymers, which compete with the amorphous aggregates. Direct injection of unfolded purified  $\gamma$ -tubulin into single-cell zebra fish embryos allowed us to relate this *in vitro* activity with the *in vivo* formation of intracellular aggregates. Injection of a CCT-binding deficient  $\gamma$ -tubulin mutant dramatically diminished the size of the intracellular aggregates, increasing the toxicity of the misfolded protein. These results point to CCT having a role in the remodeling of aggregates, constituting one of its many functions in cellular proteostasis.

### 1. Introduction

Protein aggregation is an inevitable consequence of cell existence [1]. In the cytoplasm, proteins can aggregate into amorphous, non-functional states by polymerization of monomers trapped in kinetically stable, non-native conformations, or by forming very stable amyloid-like structures. Protein aggregation can be triggered by several factors such as thermal and oxidative stress, alterations in their primary structure or in the expression of metastable gene products, and aging, among others [2–6]. Cellular toxicity is one of the most common consequences of intracellular and extracellular protein aggregation [7–10]. The response of the cell against protein aggregate toxicity lies in the removal of the aggregated protein from the cytoplasm, by forming non-toxic aggregates or inclusion bodies, or by degradation through the quality control system [6,9,11], a complex network of mechanisms that ensure the correct functionality of the proteome [12–14].

Molecular chaperones act as important modulators of protein aggregation and have been linked to the pathogenesis of a variety of protein misfolding-related disorders [15–17]. The chaperone Hsp70 [18–20] and the eukaryotic chaperonin CCT (also termed TRiC

[21–26] are prime examples. Despite the biomedical relevance of the latter, the exact role of this chaperonin in the intracellular protein aggregation process is not clear [27]. At first sight, chaperonins operate by preventing protein aggregate toxicity by sequestering misfolded proteins, avoiding their aggregation, and helping them to achieve their native state. Nevertheless, abundant evidence points towards soluble misfolded monomers or oligomers as the primary toxic agents underlying misfolding disease [15,17], while larger aggregates or their deposits may be inert or even protective [5,16,28]. Thus, one of the roles of chaperonins could be the promotion of the formation of non-toxic aggregates [23,27]. In the same way, it has been reported that CCT activity can reduce the toxicity of intracellular amyloid aggregation of huntingtin [21,23,25,29] and  $\alpha$ -synuclein [30], by altering their aggregation state. Nevertheless, most of the CCT substrate (client) proteins do not conform to any recognizable amyloid aggregation process, even though they tend to have complex topologies and a strong tendency to aggregate [24], as described for the  $\alpha/\beta$  tubulin heterodimers [31]. In this paper, we address the hypothesis that under conditions of high quantities of misfolded protein, CCT may act as a remodeling factor of aggregates of non-amyloid client proteins, reducing the

\* Corresponding author at: Las Palmeras #3425, Ñuñoa, Santiago, Chile.

E-mail address: [monaster@uchile.cl](mailto:monaster@uchile.cl) (O. Monasterio).

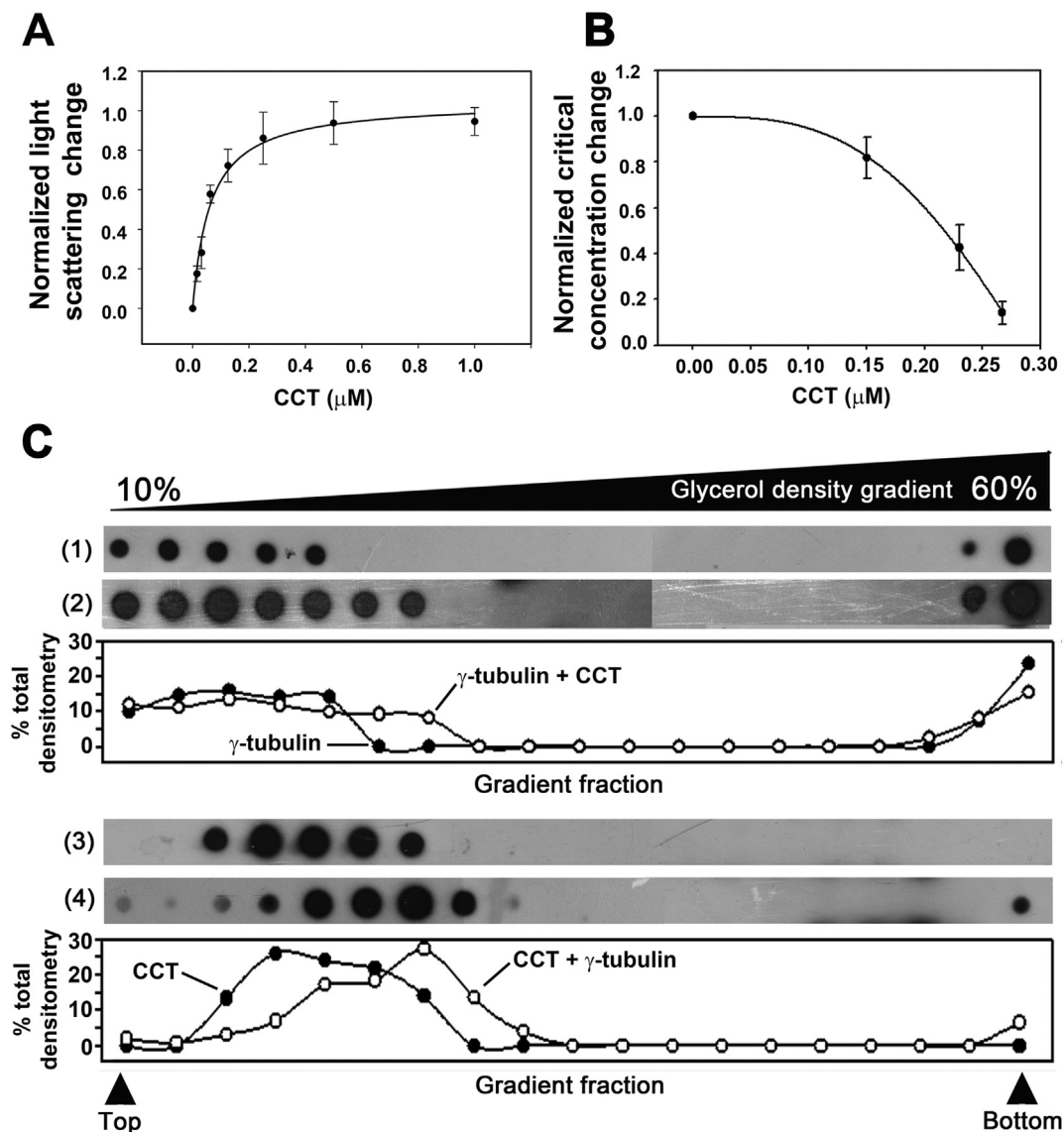


**Fig. 1.** CCT binds  $\gamma$ -tubulin monomers and induces an increase in aggregate formation.

**A)** Light scattering binding assay. A fixed amount of  $\gamma$ -tubulin ( $1\ \mu\text{M}$ ) was titrated with increasing concentrations of CCT. The  $\gamma$ -tubulin aggregation reaction was followed by light scattering at 350 nm. All measurements were performed at equilibrium and the data were corrected by the CCT scattering contribution. The data were normalized as fractional change and fitted with a one-site saturation ligand binding model. **B)** CCT effect over the apparent critical concentration ( $C_{capp}$ ) of  $\gamma$ -tubulin aggregation.  $C_{capp}$  were obtained by monitoring aggregation induction by a series of  $\gamma$ -tubulin dilutions in the presence of increasing concentrations of CCT. All reactions were performed at equilibrium and followed by light scattering at 350 nm. All data were fitted with a linear regression equation (Fig. S1D).  $C_{capp}$  were calculated from the line equations, normalized and plotted with respect to the  $\gamma$ -tubulin  $C_{capp}$  in the absence of CCT. All data were corrected by subtracting the CCT scattering contribution. Three independent experiments were averaged. Error bars indicate standard deviation. **C)** Influence of CCT over  $\gamma$ -tubulin aggregate size distribution. Glycerol gradient sedimentation was performed in order to characterize the size distribution of  $\gamma$ -tubulin aggregates in the absence (1) and the presence (2) of CCT. Co-sedimentation of CCT with  $\gamma$ -tubulin aggregates in the absence (3) and in the presence (4) of  $\gamma$ -tubulin was also investigated by analyzing the size distribution of CCT particles. The presence of  $\gamma$ -tubulin and CCT was detected by dot-blots using monoclonal antibodies against  $\gamma$ -tubulin and  $\epsilon$ -CCT. The densitometry of each dot was plotted under dot-blot rows.

cellular toxicity of the aggregate. Using  $\gamma$ -tubulin as a tubulin client model, and a multi-dimensional approach, we consistently demonstrate that CCT acts as an aggregate remodeling factor of a non-amyloid client protein, inducing the *in vitro* formation of larger fibrillar aggregates, that are associated with a reduction in toxicity in zebra fish early embryos.

## 2. Materials and methods

Recombinant  $\gamma$ -tubulin was prepared by insertion of human  $\gamma$ -tubulin 1 cDNA into a pET11a vector (Novagen®) and expression in *E. coli* BL21 (DE3) competent cells. The mutagenesis of  $\gamma$ -tubulin was performed by PCR using the pET11a- $\gamma$ -tubulin plasmid as template. The

resultant plasmids were evaluated by restriction analysis and sequencing. Recombinant  $\gamma$ -tubulin formed inclusion bodies from which the protein was purified. The protein was then dissolved using 8 M urea buffer (10 mM  $\text{Na}_2\text{S}_2\text{O}_5$ , 5 mM DDT, 20 mM Tris, pH 8) according to the method described by Sambrook et al. [32], and passed through an ion exchange (Q-Sephadex®) chromatography column and eluting with a KCl gradient (0–0.5 M). Bovine CCT was prepared from fresh tissue, as described by Llorca et al. [33] and Bertrand et al. [34].

For solution light scattering experiments, recombinant  $\gamma$ -tubulin that had been previously denatured with 6 M GdmCl was mixed with purified CCT by fast dilution in reaction buffer (5 mM  $\text{MgCl}_2$ , 150 mM NaCl, 1 mM DTT, 50 mM Tris, pH 7.2). The reactions were incubated for 30 min at 30 °C and light scattering was measured in a Shimadzu

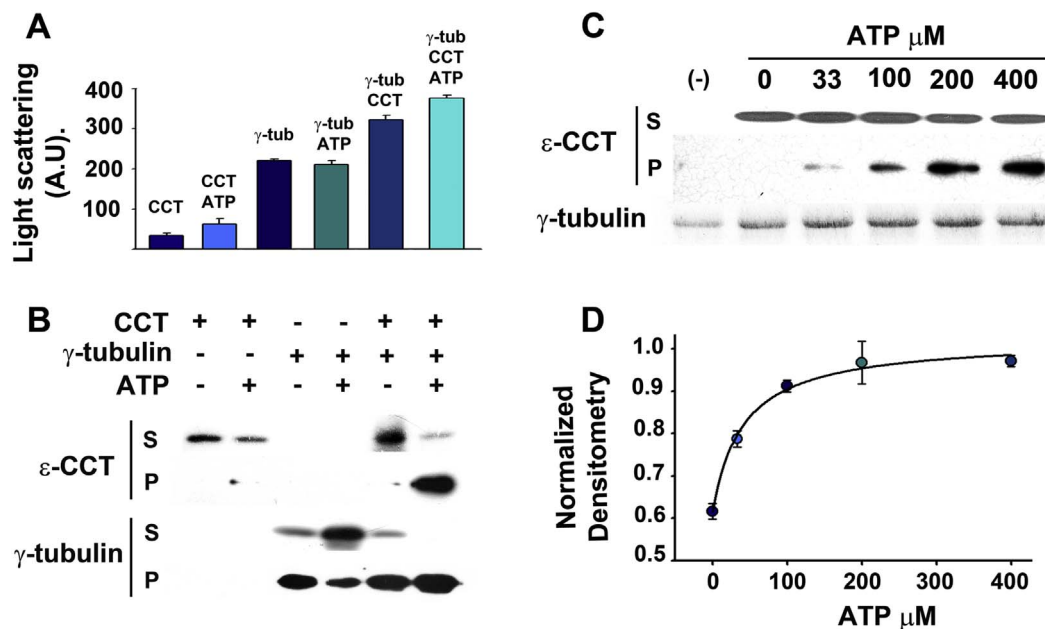


Fig. 2. Dependence on ATP of CCT-mediated  $\gamma$ -tubulin aggregation.

This reaction was analyzed by A) light scattering at 350 nm and B) co-sedimentation revealed by western-blot (WB). Supernatants (S) and pellets (P) were separated after the sedimentation (10 min at 15,000  $\times g$ ) and the presence of  $\gamma$ -tubulin (1  $\mu M$ ) and CCT (0.02  $\mu M$ ) analyzed. The induction of aggregates increases in the presence of ATP (1 mM). C) Aggregate induction reactions (1  $\mu M$   $\gamma$ -tubulin + 0.02  $\mu M$  CCT) were titrated with increasing concentrations of ATP. Aggregate formation was revealed by sedimentation (10 min at 15,000  $\times g$ ) followed by WB (for CCT) and SDS-PAGE stained with Coomassie (for  $\gamma$ -tubulin). D) ATP dependence of  $\gamma$ -tubulin aggregation induction was quantified by densitometry from SDS-PAGE stained with Coomassie blue obtained in C). Three independent experiments were averaged. Error bars indicate standard deviation.

Spectrofluorometer RF-5000 U or a Perkin-Elmer Spectrofluorometer LS50B at 350 nm. Negative controls were performed with purified CCT in the absence of recombinant  $\gamma$ -tubulin. For each measurement, the negative control value was subtracted.

For glycerol density gradients, purified CCT (0.05  $\mu M$ ) was mixed with denatured  $\gamma$ -tubulin (5  $\mu M$ ) in the reaction buffer, and incubated at 30  $^{\circ}C$  for 30 min. The solution was loaded directly in a discontinuous density gradient (10, 20, 40 and 60%) and centrifuged at 100,000  $\times g$  in a Sorvall<sup>®</sup> swinging bucket AH650 rotor during 3 h. As a negative control, CCT and  $\gamma$ -tubulin were loaded into the gradients independently. The gradients were collected in 0.2 ml fractions and subjected to dot blot analysis using monoclonal antibodies against  $\gamma$ -tubulin (SIGMA Tu88) and the  $\epsilon$ -CCT subunit (Santa Cruz Biotechnologies TCP-1 $\epsilon$  (D-6)). For co-precipitation experiments, reactions were precipitated by centrifugation at 15,000  $\times g$  during 10 min, resolved by SDS-PAGE electrophoresis, stained with Coomassie blue and finally subjected to western blot analysis.

For *in vivo* experiments, single-cell zebrafish early embryos were microinjected with 5  $\mu M$  carboxytetramethylrhodamine (TAMRA<sup>®</sup>) labeled  $\gamma$ -tubulin (final concentration). The inner cell  $\gamma$ -tubulin behavior was followed by fluorescence microscopy using an Axiovert 135 Zeiss microscope. For density gradient fractionation, 100 microinjected 4 hpf embryos were lysed in zebrafish lysis buffer (1 mM EGTA, 100 mM KCl, protease inhibitor Complete<sup>®</sup> Roche, 50 mM Hepes, pH 7.6) and cleared by centrifugation at 15,000  $\times g$ . The supernatant was fractionated in a discontinuous glycerol density gradient (5, 10, 20 and 40%) by ultracentrifugation at 100,000  $\times g$  in a Sorvall swinging bucket AH650 rotor during 4 h. The resulting gradients were separated and analyzed by western blot.

For electron microscopy,  $\gamma$ -tubulin aggregation reactions were performed in the presence or the absence of CCT and ATP. The reactions were incubated for 30 min at 30  $^{\circ}C$  as stated above, and then loaded into carbon coated copper grids (Ted Pella INC. USA.). Grids were stained with 2% uranyl acetate (w/v) for 1 min. The grids were observed in a PHILIPS TECNAI 12 BIOTWIN operated at 80 kV, at 87,000  $\times$  magnification. The micrographs were taken under low dose

conditions.

### 3. Results and discussion

The tubulin folding pathway has been extensively characterized [35–39]. The  $\alpha$ - and  $\beta$ -tubulin isoforms follow a very complex folding process [40] that includes the chaperonin CCT and more than five folding factors that act consecutively [41–43]. To our knowledge, these tubulins have never been refolded *in vitro* to their functional state in the absence of their specific folding factors. To avoid problems with other folding factors, we used  $\gamma$ -tubulin, which only requires CCT for its proper folding [37]; hence, it is a more suitable model for this study. The formation of  $\gamma$ -tubulin aggregates can be easily detected *in vitro* by light scattering (Fig. S1A). This measurement allows us to detect changes in the aggregation state since the extent of light scattering depends directly on particle size [44,45]. We expressed human  $\gamma$ -tubulin in *E. coli* as inclusion bodies, which were purified and solubilized in 6 M guanidinium chloride. The recombinant human  $\gamma$ -tubulin was very prone to aggregation in the absence of denaturant agents (see Fig. S1A). The aggregation showed an apparent critical concentration behavior with a value of  $33.1 \pm 4.2$  nM. The term apparent critical concentration ( $C_{c,app}$ ) will be used as the sum of all remaining soluble species that do not produce light scattering (at the wavelength used) in a protein aggregation reaction [46,47].  $C_{c,app}$  is estimated directly by the intersection of linear curves with the abscissa axis, at a zero value of light scattering (ordinate) (Fig. S1D).

CCT complexes were purified from bovine testis. In order to determine whether bovine purified CCT effectively binds denatured recombinant human  $\gamma$ -tubulin, we performed a two-dimensional gel electrophoresis assay (Fig. S1B). The resulting band profiles clearly show that bovine CCT effectively binds unfolded recombinant human  $\gamma$ -tubulin.

We then performed a prevention-of-aggregation experiment [4], following the aggregation state of recombinant  $\gamma$ -tubulin by fixed angle light scattering at 350 nm in order to determine changes in the formation of  $\gamma$ -tubulin aggregates induced by the addition of CCT to the

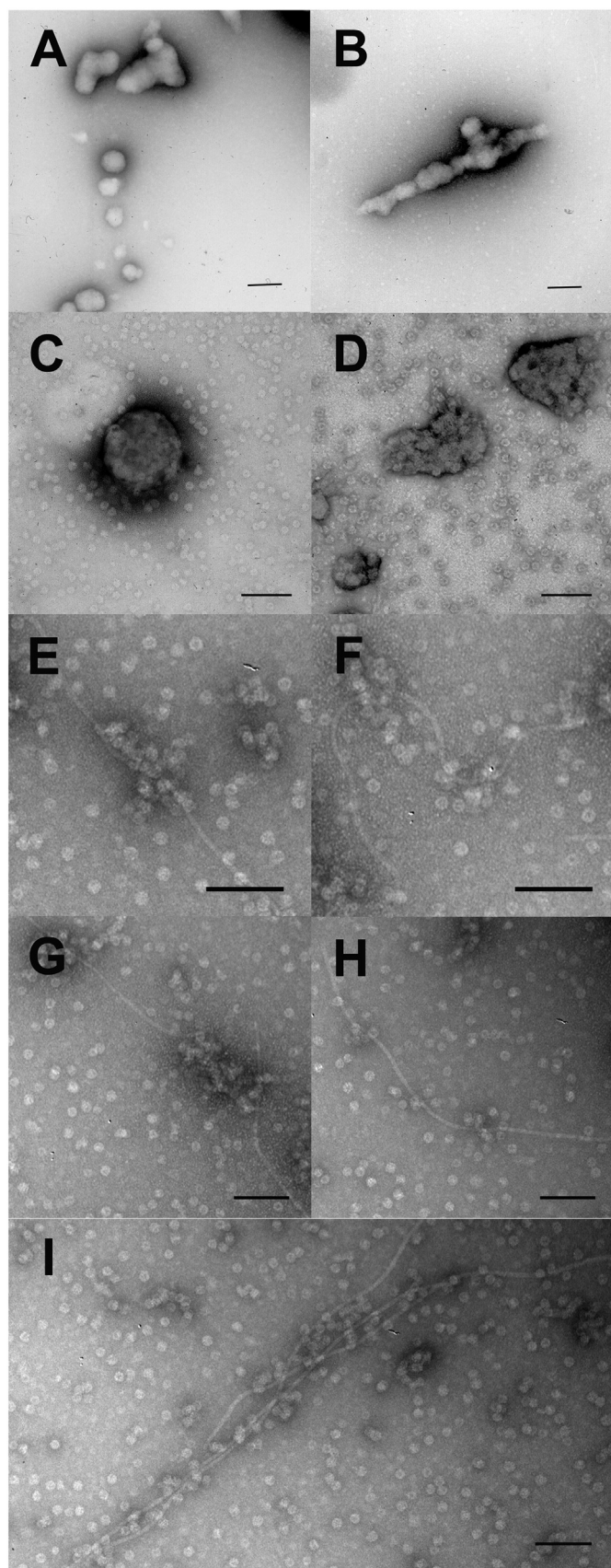


**Fig. 3.** Transmission electron micrographs of representative  $\gamma$ -tubulin aggregates induced by CCT.

A) and B)  $\gamma$ -tubulin aggregation reaction in the absence of CCT. C) and D) reactions performed using a 20:1  $\gamma$ -tubulin:CCT molar ratio (1:0.05  $\mu$ M). E) to I) reactions performed using a 100:1  $\gamma$ -tubulin:CCT molar ratio (5:0.05  $\mu$ M) plus 1 mM ATP. In all cases, the reaction mixture was prepared by fast dilution and incubated during 30 min at 30 °C. The samples were not filtered before grid preparation. Scale bars = 100 nm.

reaction. A fixed concentration of denatured soluble  $\gamma$ -tubulin was titrated by increasing concentrations of CCT in independent fast dilution experiments (see [Methods](#)). Surprisingly, the results consistently showed that the addition of CCT to the  $\gamma$ -tubulin aggregation reaction increased the light scattering signal ([Fig. 1A](#)), until it reached saturation. The calculated parameters of the reaction were  $K_{50} = 62.3 \pm 8.5$  nM, assuming one binding site for  $\gamma$ -tubulin in the same population of CCT molecules, whose binding followed a hyperbolic behavior. Higher  $\gamma$ -tubulin concentrations only increased the signal intensity without changing the behavior of the aggregation curves ([Fig. S1C](#)). Nevertheless, under a low molar ratio of  $\gamma$ -tubulin:CCT ( $\leq 1:1$ ) (indicated by black arrows in [Fig. S1C](#)), aggregation diminished as shown by the small decrease in light scattering. This result is compatible with a prevention of  $\gamma$ -tubulin aggregation at sub stoichiometric  $\gamma$ -tubulin concentrations. On the other hand, at a high concentration of misfolded protein, addition of CCT induces an increment in the mass or the size of the  $\gamma$ -tubulin aggregates.

[Fig. 1B](#) shows that the critical concentration of  $\gamma$ -tubulin aggregation decreases as CCT is added to the reaction. It is interesting to note that the  $C_{c,app}$  decreases without altering the slope of the curves (see [Fig. S1D](#)), consistently suggesting that CCT interacts with denatured monomeric  $\gamma$ -tubulin, probably favoring the aggregation-prone intermediates.

We performed an equilibrium sedimentation assay in glycerol gradients (10–60%) to characterize the relative density of the  $\gamma$ -tubulin aggregates formed during the aggregation reaction. The results show that  $\gamma$ -tubulin has a bimodal distribution in the gradient ([Fig. 1C](#)), with a lighter population (probably made of soluble monomers and small aggregates) and a denser population (made of larger aggregates). Addition of CCT to the reaction in a 100:1 (tubulin:CCT) molar relation displaces the lower population of  $\gamma$ -tubulin to higher densities ([Fig. 1C](#); top fractions). In the same manner, CCT consistently moves towards denser fractions in the presence of  $\gamma$ -tubulin, even reaching the bottom in small portions ([Fig. 1C](#); bottom fractions). This result indicates that CCT induces  $\gamma$ -tubulin aggregates by favoring the intermediates, which in some cases remain bound to the chaperonin. A similar effect of CCT binding to protein aggregates was observed using yeast protein aggregate models [48]. Moreover, the GroEl chaperonin stimulates the aggregation of the prion protein Het-s, as well as binding and decorating the aggregates formed [49].

It has been well described that CCT subunits bind and hydrolyze ATP during the folding reaction [50–57]. Therefore, we asked whether addition of ATP could modify the induction of aggregation. Experiments using light scattering ([Fig. 2A](#)) and sedimentation ([Fig. 2B](#)) reveal a significant increase in the extent of aggregation when 1 mM ATP is added to the reaction. Moreover, CCT- $\gamma$ -tubulin co-sedimentation also increases in the presence of ATP. Titration with ATP observed by sedimentation confirms this latter result, showing a hyperbolic behavior with a  $K_{50}$  of  $40.9 \pm 9.2$   $\mu$ M ([Fig. 2C](#) and D), a value close to the binding constant ( $K_d = 62.9 \pm 23$   $\mu$ M) obtained in the CCT-ATP binding experiments (see [Fig. S2](#)).

We then analyzed the  $\gamma$ -tubulin aggregation effect, both in the absence and the presence of CCT, using electron microscopy. Aliquots of the different samples were negatively stained using uranyl acetate and observed in the electron microscope ([Fig. 3](#)). In the absence of CCT, most  $\gamma$ -tubulin was found as large, amorphous aggregates ([Fig. 3A–B](#)), in accordance with the results shown previously. The presence of CCT had only minor effects on the size and shape of the  $\gamma$ -tubulin aggregates

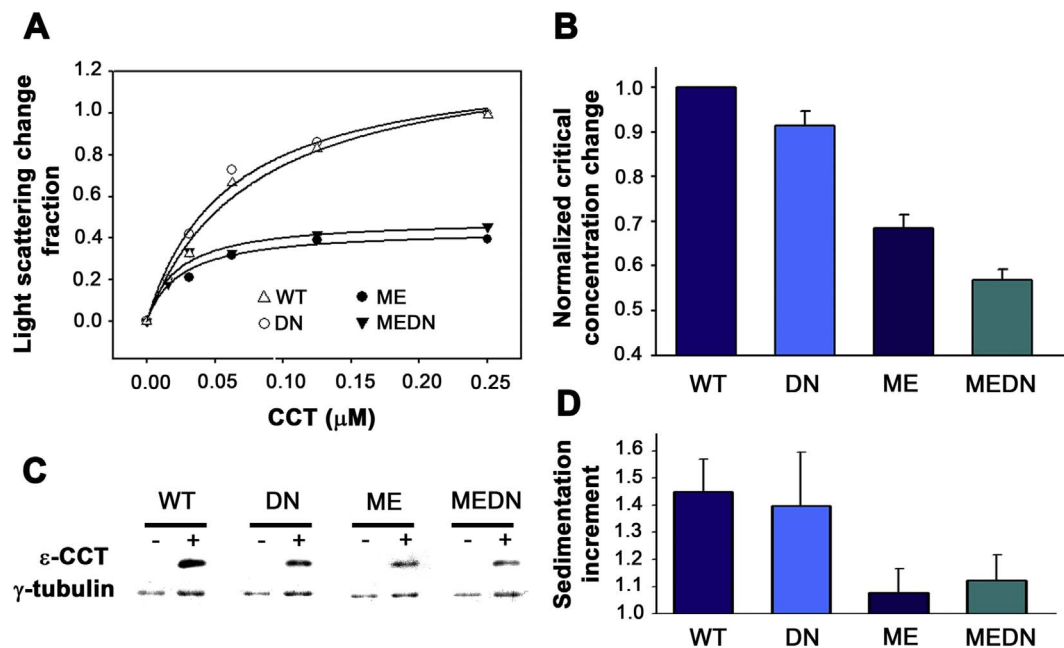


**Fig. 4.** The ME mutation in the  $\gamma$ -tubulin T7 loop significantly decreases CCT-induced aggregation.

A) Binding assays followed by light scattering. A fixed amount (0.1 mM) of wild type  $\gamma$ -tubulin (WT) and the DN, ME and MEDN mutants was titrated with increasing amounts of CCT. Aggregate formation was followed by light scattering at 350 nm. All measurements were performed at equilibrium and the CCT scattering contribution was subtracted. B) CCT effect over the  $C_{capp}$  of mutant  $\gamma$ -tubulin aggregation. Increasing concentrations of  $\gamma$ -tubulin were induced to aggregate in the absence and the presence of a fixed concentration of CCT (0.02  $\mu$ M). The change in the  $C_{capp}$  of the  $\gamma$ -tubulin CCT-induced aggregation was calculated for each mutant and normalized with respect to the WT  $C_{capp}$  change. All reactions were done at equilibrium and followed by light scattering at 350 nm. C) Sedimentation experiment of mutant  $\gamma$ -tubulin induced to aggregate in the presence (0.02  $\mu$ M) or the absence of CCT. The pellets were revealed by western blotting against  $\epsilon$ -CCT and Coomassie blue for  $\gamma$ -tubulin detection. D) The  $\gamma$ -tubulin signal of three independent sedimentation experiments was analyzed by densitometry. ME and MEDN mutants precipitated significantly less than the WT protein. Mutant DN did not show any differences compared to WT. Error bars indicate standard deviation.

(Fig. 3C–D). However, the incubation of  $\gamma$ -tubulin with CCT and ATP induced a major change: together with some amorphous  $\gamma$ -tubulin aggregates, long and thin ( $6.7 \pm 0.9$  nm;  $n = 108$ ) fibers were also observed (Fig. 3G–H). This behavior is related with a change of shape and a slight rise in intensity in the emission spectra of the amyloidogenic probe Thioflavin T, but not with Congo red (Fig. S3). We ruled out the possibility that the  $\gamma$ -tubulin fibers were made from a native protein conformation for two main reasons: firstly, the reactions were performed in the absence of GTP, essential for tubulin folding and polymerization. Secondly, different *in vitro* refolding experiments of  $\gamma$ -tubulin performed in the presence of CCT gave monomeric forms of  $\gamma$ -tubulin [37], rather than filaments. To our knowledge, this is the first time that long filament-shaped polymers formed from purified or re-natured  $\gamma$ -tubulin, have been reported. The absence of GTPase activity of these filaments, discards the presence of native  $\gamma$ -tubulin.

The CCT-induced formation of  $\gamma$ -tubulin aggregates was analyzed by  $\gamma$ -tubulin mutation experiments. It has been hypothesized that the T7 and M loops, which are involved in tubulin-tubulin longitudinal and lateral interactions, respectively [58,59], also participate in the recognition of tubulin by CCT [34,36]. Based on this information and on the analysis of the sequence of both loops, we decided to introduce a point mutation near the middle of the T7 loop, by replacing the hydrophobic Met<sub>248</sub> with a negatively-charged Glu (ME mutant). Likewise, we considered aspartic D<sub>278</sub> as one of the more conserved residues in the M loop sequence (Fig. S4), located almost in the middle of the M loop structure. We decided to remove this charged amino acid and replace it with Asn (DN mutant). We also constructed a double mutant (MEDN mutant).

Three different approaches were performed: In the first, a prevention of  $\gamma$ -tubulin aggregation experiment was carried out with the mutants ME, DN and MEDN in the presence of increasing concentrations of CCT (Fig. 4A). In these experiments, ME and MEDN mutants consistently diminished the aggregation induced by CCT (about 30% of

the total effect) compared with DN and WT proteins. A second experiment (Fig. 4B), designed to observe the ability of CCT to decrease the  $C_{capp}$  of the aggregation of the mutant proteins, again showed a significant decrease in the effect of CCT over the  $C_{capp}$  of ME and MEDN proteins. However, such conditions did not affect the aggregation of the DN mutant, which was very similar to that of the wild type protein. It is important to note that the  $C_{capp}$  of all proteins was about the same in the absence of CCT (Fig. S4B). This latter observation indicates that mutations in the T7 or the M loop, do not cause by themselves any effects on  $\gamma$ -tubulin aggregation, yet they do alter CCT-induced aggregation. In the third experiment, aggregate formation was evaluated by sedimentation. The results consistently show that mutations ME and MEDN significantly diminish CCT-induced  $\gamma$ -tubulin aggregation. Altogether, these results unambiguously demonstrate that the ME mutation in the T7 loop diminishes CCT binding to  $\gamma$ -tubulin. Therefore, the observed CCT-induced  $\gamma$ -tubulin aggregation depends on specific recognition between  $\gamma$ -tubulin and the chaperonin.

We then evaluated whether the phenomenon observed *in vitro* is related to the formation of aggregates within a living cell. We took advantage of the CCT-binding deficient ME mutant and performed an experiment in which purified unfolded recombinant  $\gamma$ -tubulin was labeled with rhodamine and microinjected inside living single-cell zebrafish early embryos [60]. The behavior of the injected protein was followed by fluorescence microscopy. Fig. 5A shows two representative injected embryos during their earliest developmental stages, in which formation of large intracellular protein aggregates is evident [61]. These  $\gamma$ -tubulin aggregates resemble the well characterized perinuclear protein aggregation organelles called aggresomes [1,3].

Several embryos were injected with the ME mutant and WT unfolded  $\gamma$ -tubulin, and the presence of intracellular aggregates was registered and quantified. The results show that the injection of the ME  $\gamma$ -tubulin mutant induced the formation of aggregates in  $13.8 \pm 11.3\%$  ( $n = 42$ ) of live embryos, significantly fewer than those found for

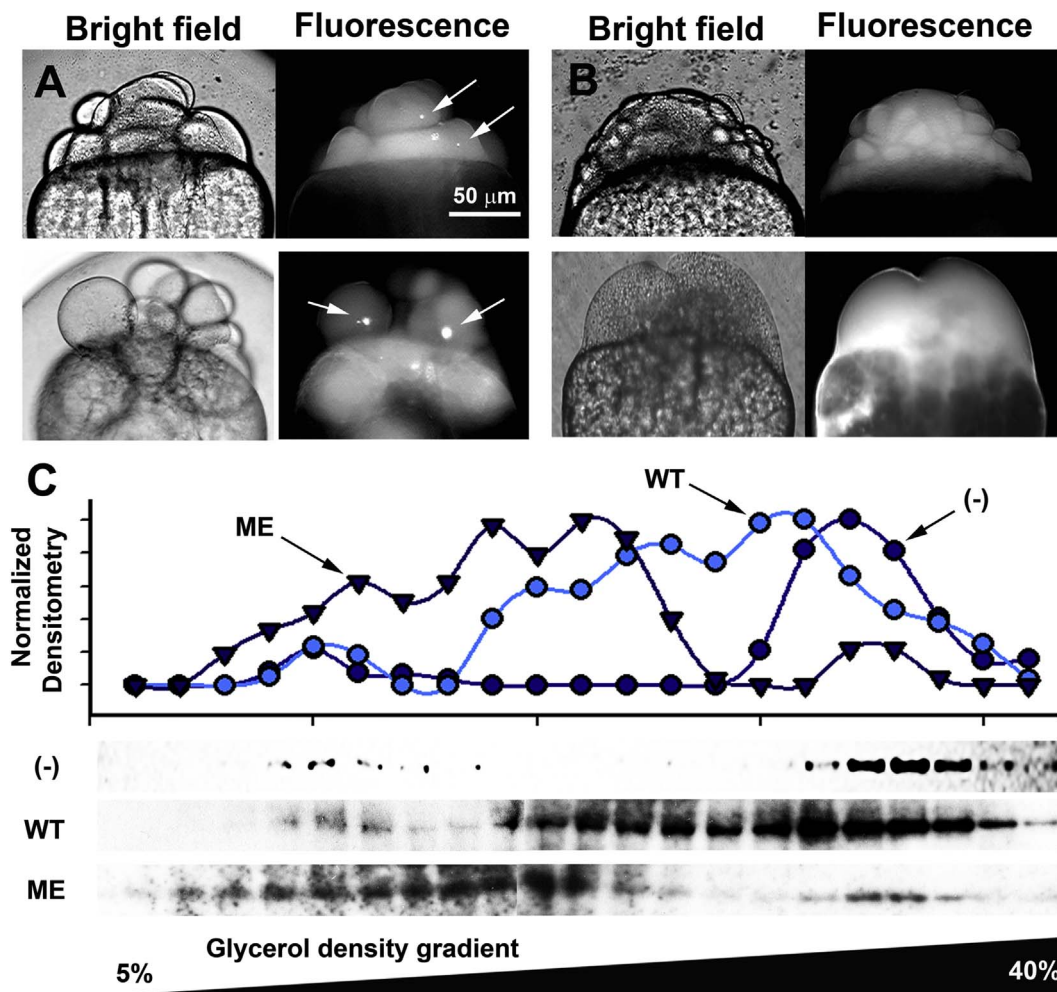


**Fig. 5.** CCT is related with the formation of intracellular  $\gamma$ -tubulin aggregates.

A) Bright field and fluorescence microscopy of two representative single-cell zebrafish embryos (2 Hours Post Fecundation (HPF)) injected with rhodamine labeled WT  $\gamma$ -tubulin. White arrows depict  $\gamma$ -tubulin aggregate formation. B) Bright field and fluorescence microscopy of two representative zebrafish embryos (2 HPF) injected with rhodamine labeled ME mutant  $\gamma$ -tubulin. C) The ME mutation in the  $\gamma$ -tubulin T7 loop significantly decreases the size of  $\gamma$ -tubulin aggregates. WT and ME  $\gamma$ -tubulin were injected into single-cell zebrafish embryos. After four hours incubation (22 °C), embryos were homogenized, cleared and separated by ultracentrifugation in a discontinuous glycerol density gradient (5–40%). The presence of  $\gamma$ -tubulin was detected by western blot. The optical density was calculated, normalized and plotted over each individual lane. As negative control (-), a non-injected embryos gradient is shown.

embryos injected with WT  $\gamma$ -tubulin ( $66.5 \pm 8.1\%$  ( $n = 53$ )) (Fig. 5B). Injection of the ME mutant diminished the survival of the embryos ( $35 \pm 10.4\%$  ( $n = 120$ )) in comparison to those injected with WT  $\gamma$ -tubulin ( $66.3 \pm 17\%$  ( $n = 80$ )) (Fig. S5), highlighting the importance of CCT in the detoxification of the intracellular protein aggregates.

Finally, we developed an ultracentrifugation experiment with the aim of qualitatively determining the relative size of the particles that constitute the intracellular  $\gamma$ -tubulin aggregates formed by WT  $\gamma$ -tubulin and the ME mutant. The injected embryos were incubated for 4 h, and then lysed, cleared by centrifugation, and the clarified lysate subjected to separation by ultracentrifugation in discontinuous density gradients. The distribution of injected WT and ME  $\gamma$ -tubulin in the gradient shows that both proteins overlap only partially with the endogenous protein (Fig. 5E), suggesting that they were not incorporated into native structures. Thus, the results unambiguously demonstrate that the injected ME mutant protein forms intracellular aggregates that are significantly smaller than those formed by WT  $\gamma$ -tubulin, confirming our *in vitro* results. Based on the latter, we propose that the detoxification of high quantities of misfolded protein mediated by CCT results in the removal of the misfolded protein, forming larger, less toxic intracellular protein aggregates.

Information concerning this effect is scarce, although there are a few reports of similar processes of aggregation for amyloidogenic

proteins that do not seem to form part of the CCT interactome [24] such as huntingtin [23] or PrP [27]. In the same way, most proteins recognized by CCT show complex topologies [24], which are especially vulnerable to aggregation [62], usually through the recognition of  $\beta$ -strand regions. This, together with interactomic information that point to CCT in the pathogenesis of amyloid diseases [26], and the cellular location of CCT in aggresomes [63], strongly suggest that CCT-mediated aggregation could be a more general process involved in the detoxification triggered by the accumulation of misfolded proteins in the cytoplasm, regardless of the nature of the aggregates (in Fig. S6, CCT also induces the aggregation and co-precipitation with rhodanase and purified  $\alpha/\beta$  tubulin heterodimers).

#### 4. Conclusion

In this study we investigated a process of aggregation mediated by CCT on one of the most important CCT client proteins, the tubulins [24], specifically  $\gamma$ -tubulin. This aggregation phenomenon is manifested as a significant increase in the amount of misfolded  $\gamma$ -tubulin aggregates, accompanied by the appearance of fibrillar aggregates. This phenomenon is shown to be ATP dependent and to some extent, sequence specific.

To address the *in vivo* implications of this effect, we performed an

assay in which we subjected zebrafish embryos to conditions of high quantities of intracellular misfolded proteins. The embryonic cells responded by generating large intracellular aggregates, very similar to the previously-described aggresomes [1]. One point mutation in a critical region of interaction between tubulin-CCT, significantly decreased the effect and increased the toxicity of the tubulin aggregates, confirming this hypothesis. Thus, the presence of an aggregate induced by CCT competes with the formation of amorphous aggregates, and could constitute a means to manage toxic intermediates and ensure cellular proteostasis. Future studies are needed to determine the molecular mechanism of this CCT function and its real implications in a cellular context.

Finally, it is obvious that the cellular functions of CCT are more complex than previously thought, and this complexity is probably related to its own complex structure [64]. The overall function and the specificity notion of type II chaperonins must be revisited for a better understanding of the mechanisms of cytoskeletal protein folding/misfolding. Interestingly, the use of single-cell zebrafish embryos as a model for *in vivo* protein aggregation assays promises to be a very useful application for the study of therapies against protein misfolding-associated diseases.

### Transparency document

The [Transparency document](#) associated with this article can be found, in online version.

### Acknowledgements

We thank the *Fondo Nacional de Ciencia y Tecnología* (Grant No 1130711), the Commission of the European Communities SFP 223431 and *Programa de formación permanente de la Fundación Carolina* C. 2011 for providing financial support for this study. We thank Michael Handford (Universidad de Chile) for language support. We thank Miguel Allende for Zebrafish facilities.

### Appendix A. Supplementary data

Supplementary data to this article can be found online at <https://doi.org/10.1016/j.bbapap.2018.01.007>.

### References

- [1] R.R. Kopito, Aggresomes, inclusion bodies and protein aggregation, *Trends Cell Biol.* 10 (2000) 524–530.
- [2] W.E. Balch, Adapting proteostasis for disease intervention, *Science* 916 (2011) 916–919.
- [3] R. Garcia-Mata, Y.-S. Gao, E. Sztul, Hassles with taking out the garbage: aggravating aggresomes, *Traffic (Copenhagen, Denmark)* 3 (2002) 388–396.
- [4] F. Weber, M. Hayer-Hartl, Prevention of rhodanese aggregation by the chaperonin GroEL, *Methods Mol. Biol.* 140 (2000) 111–115.
- [5] J.A. Johnston, M.E. Illing, R.R. Kopito, Cytoplasmic dynein/dynactin mediates the assembly of aggresomes, *Cell Motil. Cytoskeleton* 53 (2002) 26–38.
- [6] S. Wickner, M.R. Maurizi, S. Gottesman, Posttranslational quality control: folding, refolding, and degrading proteins, *Science* 286 (1999) 1888–1893.
- [7] N.V. Dovidchenko, E.I. Leonova, O.V. Galzitskaya, Mechanisms of amyloid fibril formation, *Biochem. Mosc.* 79 (2014) 1515–1527.
- [8] C. Frieden, Protein aggregation processes: in search of the mechanism, *Protein Sci.* 16 (2007) 2334–2344.
- [9] T.P.J. Knowles, M. Vendruscolo, C.M. Dobson, The amyloid state and its association with protein misfolding diseases, *Nat. Rev. Mol. Cell Biol.* 15 (2014) 384–396.
- [10] R. Tycko, Amyloid polymorphism: structural basis and neurobiological relevance, *Neuron* 86 (2015) 632–645.
- [11] D. Kaganovich, R. Kopito, J. Frydman, Misfolded proteins partition between two distinct quality control compartments, *Nature* 454 (2008) 1088–1095.
- [12] J. Labbadia, R.I. Morimoto, The biology of Proteostasis in aging and disease, *Annu. Rev. Biochem.* 84 (2015) 435–464.
- [13] F.U. Hartl, A. Bracher, M. Hayer-Hartl, Molecular chaperones in protein folding and proteostasis, *Nature* 475 (2011) 324–332.
- [14] K.R. Brandvold, R.I. Morimoto, The chemical biology of molecular chaperones—implications for modulation of proteostasis, *J. Mol. Biol.* 427 (2015) 2931–2947.
- [15] P.J. Muchowski, J.L. Wacker, Modulation of neurodegeneration by molecular chaperones, *Nat. Rev. Neurosci.* 6 (2005) 11–22.
- [16] J.A. Olzmann, L. Li, L.S. Chin, Aggresome formation and neurodegenerative diseases: therapeutic implications, *Curr. Med. Chem.* 15 (2008) 47–60.
- [17] S.A. Broadley, F.U. Hartl, The role of molecular chaperones in human misfolding diseases, *FEBS Lett.* 583 (2009) 2647–2653.
- [18] A. Mogk, E. Kummer, B. Bukau, Cooperation of Hsp70 and Hsp100 chaperone machines in protein disaggregation, *Front. Mol. Biosci.* 2 (2015) 1–10.
- [19] K.C. Luk, I.P. Mills, J.Q. Trojanowski, V.M.Y. Lee, Interactions between Hsp70 and the hydrophobic core of  $\alpha$ -synuclein inhibit fibril assembly, *Biochemistry* 47 (2008) 12614–12625.
- [20] C.G. Evans, S. Wisén, J.E. Gestwicki, Heat shock proteins 70 and 90 inhibit early stages of amyloid  $\beta$ -(1–42) aggregation *in vitro*, *J. Biol. Chem.* 281 (2006) 33182–33191.
- [21] S. Tam, C. Spiess, W. Auyeung, L. Joachimiak, B. Chen, M. a Poirier, J. Frydman, The chaperonin Tric blocks a huntingtin sequence element that promotes the conformational switch to aggregation, *Nat. Struct. Mol. Biol.* 16 (2009) 1279–1285.
- [22] S. Tam, R. Geller, C. Spiess, J. Frydman, The chaperonin Tric controls polyglutamine aggregation and toxicity through subunit-specific interactions, *Nat. Cell Biol.* 8 (2006) 1155–1162.
- [23] C. Behrends, C.a. Langer, R. Boteva, U.M. Böttcher, M.J. Stemp, G. Schaffar, B.V. Rao, A. Giese, H. Kretzschmar, K. Siegers, F.U. Hartl, Chaperonin Tric promotes the assembly of polyQ expansion proteins into nontoxic oligomers, *Mol. Cell Biol.* 23 (2006) 887–897.
- [24] A.Y. Yam, Y. Xia, H.-T.J. Lin, A. Burlingame, M. Gerstein, J. Frydman, Defining the Tric/CCT interactome links chaperonin function to stabilization of newly made proteins with complex topologies, *Nat. Struct. Mol. Biol.* 15 (2008) 1255–1262.
- [25] A. Kitamura, H. Kubota, C.-G. Pack, G. Matsumoto, S. Hirayama, Y. Takahashi, H. Kimura, M. Kinjo, R.I. Morimoto, K. Nagata, Cytosolic chaperonin prevents polyglutamine toxicity with altering the aggregation state, *Nat. Cell Biol.* 8 (2006) 1163–1170.
- [26] E. Khabirova, A. Moloney, S.J. Marciniak, J. Williams, D.A. Lomas, S.G. Oliver, G. Favrin, D.B. Sattelle, D.C. Crowther, The Tric/CCT chaperone is implicated in Alzheimer's disease based on patient GWAS and an RNAi screen in  $A\beta$ -expressing *Caenorhabditis elegans*, *PLoS One* 9 (2014) 1–13.
- [27] G.G. Kiselev, I.N. Naletova, E.V. Sheval, Y.Y. Stroylova, E.V. Schmalhausen, T. Haertlé, V.I. Muronetz, Chaperonins induce an amyloid-like transformation of ovine prion protein: the fundamental difference in action between eukaryotic Tric and bacterial GroEL, *Biochim. Biophys. Acta, Proteins Proteomics* 1814 (2011) 1730–1738.
- [28] E. Swinnen, S. Büttner, T.F. Outeiro, M. Galas, F. Madeo, J. Winderickx, V. Fransens, Aggresome formation and segregation of inclusions influence toxicity of  $\alpha$ -synuclein and synphilin-1 in yeast, *Biochem. Soc. Trans.* 39 (2011) 1476–1481.
- [29] K.L. Sugars, D.C. Rubinsztein, Transcriptional abnormalities in Huntington disease, *Trends Genet.* 19 (2003) 233–238.
- [30] B. Sot, A. Rubio-Muñoz, A. Leal-Quintero, J. Martínez-Sabando, M. Marcilla, C. Roodveldt, J.M. Valpuesta, The chaperonin CCT inhibits assembly of  $\alpha$ -synuclein amyloid fibrils by a specific, conformation-dependent interaction, *Sci. Rep.* 7 (2017) 40859.
- [31] V. Prakash, S.N. Timasheff, Aging of tubulin at neutral pH, *J. Mol. Biol.* 160 (1982) 499–515.
- [32] J. Sambrook, E. Fritsch, T. Maniatis, *Molecular Cloning: A Laboratory Manual*, 2nd ed., Cold Spring Harbor, NY USA, 1989.
- [33] O. Llorca, E.A. McCormack, G. Hynes, J. Grantham, J. Cordell, J.L. Carrascosa, K.R. Willison, J.J. Fernandez, J.M. Valpuesta, Eukaryotic type II chaperonin CCT interacts with actin through specific subunits, *Nature* 402 (1999) 693–696.
- [34] S. Bertrand, I. Barthelemy, M.A. Oliva, J.L. Carrascosa, J.M. Andreu, J.M. Valpuesta, Folding, stability and polymerization properties of FtsZ chimeras with inserted tubulin loops involved in the interaction with the cytosolic chaperonin CCT and in microtubule formation, *J. Mol. Biol.* 346 (2005) 319–330.
- [35] M.B. Yaffe, G.W. Farr, D. Miklos, A.L. Horwich, M.L. Sternlicht, H. Sternlicht, TCP1 complex is a molecular chaperone in tubulin biogenesis, *Nature* 358 (1992) 245–248.
- [36] O. Llorca, K.R. Willison, Analysis of the interaction between the eukaryotic chaperonin CCT and its substrates actin and tubulin, *J. Struct. Biol.* 135 (2001) 205–218.
- [37] R. Melki, I.E. Vainberg, R.L. Chow, N.J. Cowan, Chaperonin-mediated folding of vertebrate actin-related protein and  $\gamma$ -tubulin, *J. Cell Biol.* 122 (1993) 1301–1310.
- [38] M. Ritco-Vonsovici, K.R. Willison, Defining the eukaryotic cytosolic chaperonin-binding sites in human tubulins, *J. Mol. Biol.* 304 (2000) 81–98.
- [39] P.C. Stirling, J. Cuéllar, G.A. Alfaro, F. El Khadali, C.T. Beh, J.M. Valpuesta, R. Melki, M.R. Leroux, PhLP3 modulates CCT-mediated actin and tubulin folding via ternary complexes with substrates, *J. Biol. Chem.* 281 (2006) 7012–7021.
- [40] S.A. Lewis, G. Tian, N.J. Cowan, The alpha- and beta-tubulin folding pathways, *Trends Cell Biol.* 7 (1997) 479–484.
- [41] G. Tian, Y. Huang, H. Rommelaere, J. Vandekerckhove, C. Ampe, N.J. Cowan, Pathway leading to correctly folded  $\beta$ -tubulin, *Cell* 86 (1996) 287–296.
- [42] G. Tian, N.J. Cowan, Tubulin-specific chaperones: components of a molecular machine that assembles the  $\alpha/\beta$  heterodimer, *Methods Cell Biol.* 115 (2013) 155–171.
- [43] M. Lopez-Fanarraga, J. Avila, A. Guasch, M. Coll, J.C. Zabala, Review: post-chaperonin tubulin folding cofactors and their role in microtubule dynamics, *J. Struct. Biol.* 135 (2001) 219–229.
- [44] F. Gaskin, C.R. Cantor, M.L. Shelanski, Turbidimetric studies of the *in vitro* assembly and disassembly of porcine neurotubules, *J. Mol. Biol.* 89 (1974) 737–740.
- [45] B.J. Berne, Interpretation of the light scattering from long rods, *J. Mol. Biol.* 89 (1974) 755–758.

- [46] B. O'Nuallain, S. Shivaprasad, I. Kheterpal, R. Wetzel, Thermodynamics of A $\beta$ (1-40) amyloid fibril elongation, *Biochemistry* 44 (2005) 12709–12718.
- [47] K. Ozaki, S. Hatano, Mechanism of regulation of actin polymerization by Physarum profilin, *J. Cell Biol.* 98 (1984) 1919–1925.
- [48] M. Nadler-Holly, M. Breker, R. Gruber, A. Azia, M. Gymrek, M. Eisenstein, K.R. Willison, M. Schuldiner, A. Horovitz, Interactions of subunit CCT3 in the yeast chaperonin CCT/TRiC with Q/N-rich proteins revealed by high-throughput microscopy analysis, *Proc. Natl. Acad. Sci.* 109 (2012) 18833–18838.
- [49] M.A. Wälti, T. Schmidt, D.T. Murray, H. Wang, J.E. Hinshaw, G.M. Clore, Chaperonin GroEL accelerates protofibril formation and decorates fibrils of the Het-s prion protein, *Proc. Natl. Acad. Sci.* 201711645 (2017).
- [50] M.A. Kabir, W. Uddin, A. Narayanan, P.K. Reddy, M.A. Jairajpuri, F. Sherman, Z. Ahmad, Functional subunits of eukaryotic chaperonin CCT/TRiC in protein folding, *J. Amino Acids* 2011 (2011) 1–16.
- [51] A.S. Meyer, J.R. Gillespie, D. Walther, I.S. Millet, S. Doniach, J. Frydman, Closing the folding chamber of the eukaryotic chaperonin requires the transition state of ATP hydrolysis, *Cell* 113 (2003) 369–381.
- [52] C.R. Booth, A.S. Meyer, Y. Cong, M. Topf, A. Sali, S.J. Ludtke, W. Chiu, J. Frydman, Mechanism of lid closure in the eukaryotic chaperonin TRiC/CCT, *Nat. Struct. Mol. Biol.* 15 (2008) 746–753.
- [53] I. Gutsche, J. Holzinger, M. Rößle, H. Heumann, W. Baumeister, R.P. May, Conformational rearrangements of an archaeal chaperonin upon ATPase cycling, *Curr. Biol.* 10 (2000) 405–408.
- [54] L. Skjærven, J. Cuellar, A. Martinez, J.M. Valpuesta, Dynamics, flexibility, and allostery in molecular chaperonins, *FEBS Lett.* 589 (2015) 2522–2532.
- [55] C. Spiess, A.S. Meyer, S. Reissmann, J. Frydman, Mechanism of the eukaryotic chaperonin: protein folding in the chamber of secrets, *Trends Cell Biol.* 14 (2004) 598–604.
- [56] A. Horovitz, K.R. Willison, Allosteric regulation of chaperonins, *Curr. Opin. Struct. Biol.* 15 (2005) 646–651.
- [57] H. Yébenes, P. Mesa, I.G. Muñoz, G. Montoya, J.M. Valpuesta, Chaperonins: two rings for folding, *Trends Biochem. Sci.* 36 (2011) 424–432.
- [58] H. Li, D.J. DeRosier, W.V. Nicholson, E. Nogales, K.H. Downing, Microtubule structure at 8 Å resolution, *Structure* 10 (2002) 1317–1328.
- [59] J. Löwe, H. Li, K.H. Downing, E. Nogales, Refined structure of alpha beta-tubulin at 3.5 Å resolution, *J. Mol. Biol.* 313 (2001) 1045–1057.
- [60] C. Kimmel, Genetics and early development of zebrafish, *Trends Genet.* 5 (1989) 283–288.
- [61] K. Bersuker, M. Brandeis, R.R. Kopito, Protein misfolding specifies recruitment to cytoplasmic inclusion bodies, *J. Cell Biol.* 213 (2016) 229–241.
- [62] A.J. Baldwin, T.P.J. Knowles, G.G. Tartaglia, A.W. Fitzpatrick, G.L. Devlin, S.L. Shammah, C.A. Waudby, M.F. Mossuto, S. Meehan, S.L. Gras, J. Christodoulou, S.J. Anthony-cahill, P.D. Barker, M. Vendruscolo, C.M. Dobson, Metastability of native proteins and the phenomenon of amyloid formation, *J. Am. Chem. Soc.* 133 (2011) 14160–14163.
- [63] R. García-Mata, Z. Beböök, E.J. Sorscher, E.S. Sztul, Characterization and dynamics of aggregate formation by a cytosolic GFP-chimera, *J. Cell Biol.* 146 (1999) 1239–1254.
- [64] N. Kalisman, G.F. Schröder, M. Levitt, The crystal structures of the eukaryotic chaperonin CCT reveal its functional partitioning, *Structure* 21 (2013) 540–549.